ME30030 FEA Coursework Assignment 2022

Candidate Number: 12264
Chosen Component: Squat Rack Safety Bar
FEA software used: Autodesk Inventor Professional 2022

Part 1: Component description and two-dimensional idealisation

2D idealisation: Plane Stress

Component description

In this Finite Element Analysis, a squat-rack safety bar was chosen as the component to be modelled.

An important component in the squat rack, the safety bar is crucial to ensuring the user's safety, and is placed such that if the user were to 'fail' a movement, the barbell being used would be 'caught' by the arms; such that the user would not be dangerously pinned beneath the weight(Refer to Figure 1).

The geometry of the bar being analysed made by LIFEFITNESS (LIFEFITNESS, 2021)*, consists of a main rectangular cross-section with of dimensions of 60mm x 75mm. At the either end of this section, there is a cylindrical protrusion of 30mm diameter, with which the bar is hooked onto the main squat rack.*

2D idealisation

(Turn overleaf for relevant Figure)

For this study, plane-stress was chosen as a 2D idealisation, where it is assumed that stresses act along only two dimensions ($\sigma_x, \sigma_y, \tau_{xy} \neq 0$), and that there is no stress in the third dimension ($\sigma_z, \tau_{yz}, \tau_{zx} = 0$). (Pegg, 2022). 2D stress was chosen as the bars thickness (60mm) is negligible when compared to its length (900mm). The model's thickness was assumed to be uniform throughout.

Safety bars are typically made of cast steel (Poirier-Leroy, n.d.), with the specific makeup of the material depending on the product's brand, model, etc. As such, the Young's modulus and Poisson's ratio were taken to be the average values of 200 GPa and 0.265 respectively, as they lie reasonably within the range of values for cast steel. The yield strength was taken to be 200 MPa, lying at the lower end of the of values provided for cast steel. (THOMASNET, n.d).

In order to reduce the complexity of the model, the cross-section of the bar was halved, and the corresponding point load was also halved to account for this.

Figure 1: Top: An image of the safety bar. Bottom: 2D idealisation of half a safety bar with main dimensions.

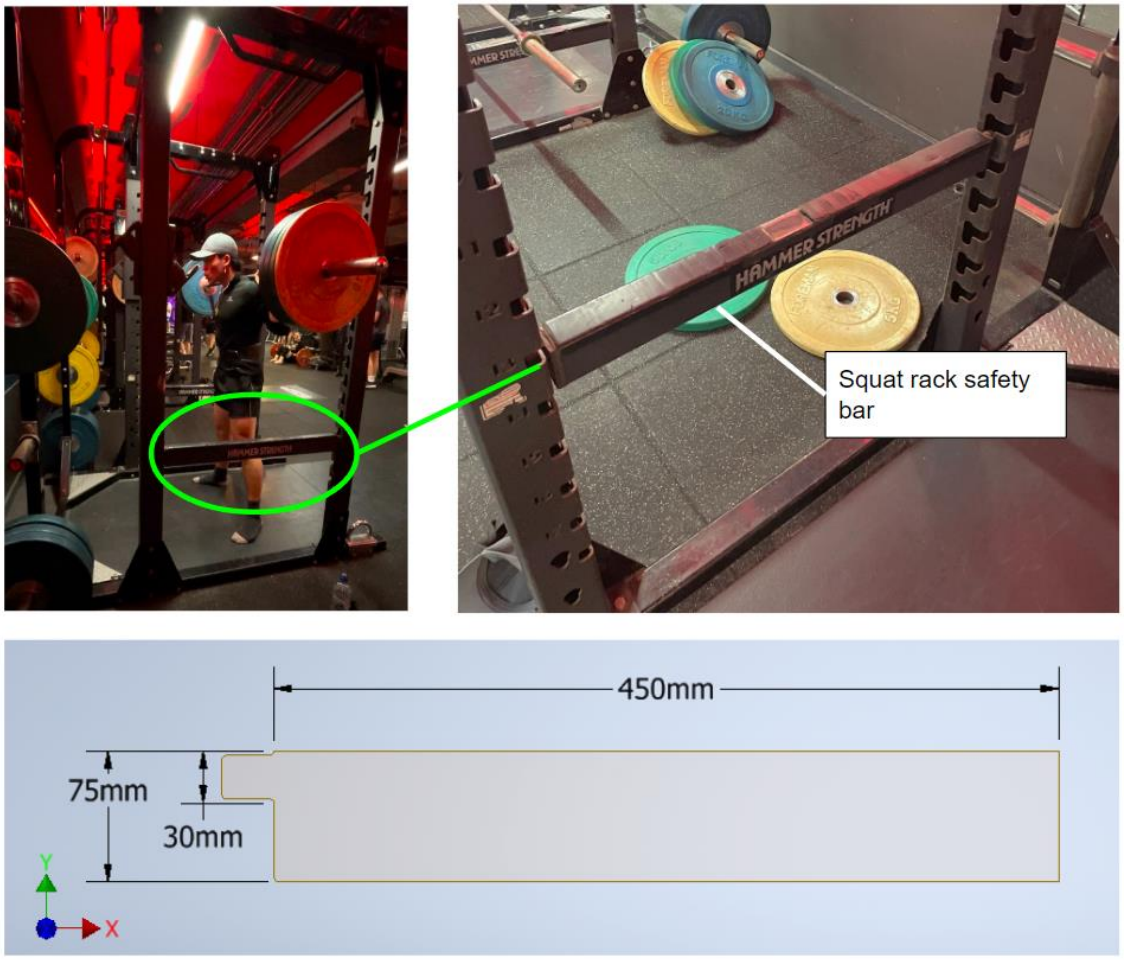

Part 2: Boundary conditions

Constraints

Referring to Figure 2:

- Point A: At this node, the assumption was made that it is a pin joint. As such, it was constrained tangentially, but not rotationally
- Point B: In order to ensure accuracy in the computed results, an x-symmetric constraint was applied at this face(As the model only represents 'half' a bar)

Applied load

To calculate the magnitude of the applied load, the product's advertised working weight of 388 kg (LIFEFITNESS, 2021) was used. Assuming the weight to be resting centrally on top of two safety bars typically installed on a squat rack, the expected acting on the model was calculated to be approximately 1000N.

Due to the large uncertainty in this value, it was decided that a magnitude of 1500N would be used as a conservative estimate.

This load was modelled as a point load at the centre of the bar(Point C on Figure 2), acting uniaxially in the negative y direction.

Physically, this represents a loading case where a barbell with 388kg loaded onto it is resting on two safety bars.

Figure 2: The boundary conditions used in the FEA model. Point A was constrained in all three tangential directions(x, y, and z), but allowed to rotate freely. Face BC has an x-symmetric constrained applied to it, and a uniaxial point load of 1500N is applied at point B in the negative y-direction

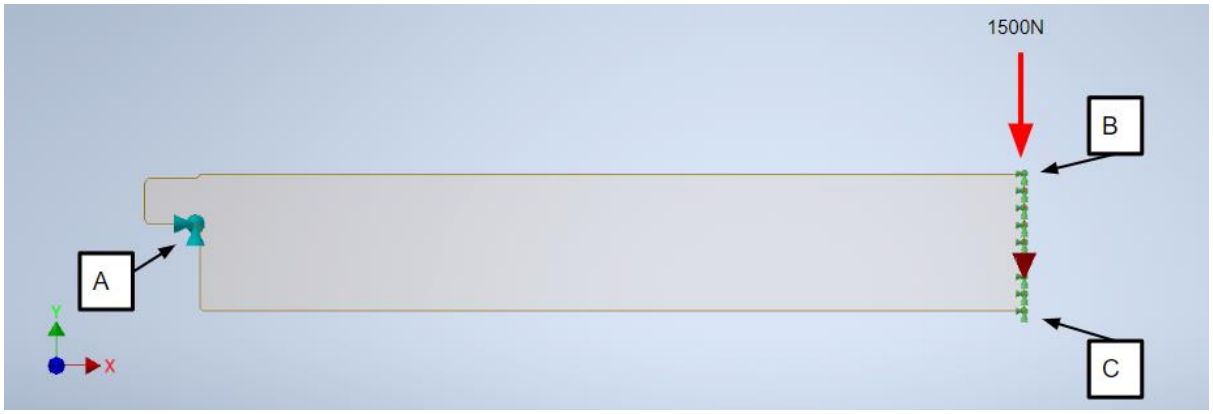

Table of input parameters:

Young's modulus:	200 Gpa
Poisson's ratio:	0.265
Applied load:	-1500N(Based on specs provided on Hammer Strength Website)
Yield Strength:	200 MPa(conservative estimate)

(THOMASNET, n.d), (The Engineering Toolbox., n.d), (Civil's Guide, 2021)

Part 3: Mesh

Element type:	Triangular - parabolic
Element size:	0.8mm

3.1. Mesh Selection

For the mesh in this FEA, a parabolic triangular mesh was selected.

The mesh was chosen to be parabolic as opposed to linear due the larger number of nodes. This allows for a better representation of the component's geometry, and as such increases the overall accuracy.

A triangular mesh was chosen over a quadrilateral mesh due to the model's geometry. As one of the major points of interest is a sharp corner (Point A on Figure 2), a triangular mesh is appropriate as they are generally better at modelling corners than a quadrilateral one (Haimes and Docampo-Sánchez, J, 2019).

It should be noted that in selecting a triangular mesh, there is a trade-off in computational efficiency due to their lower aspect ratio. i.e. a larger number of triangular elements are needed to represent a component, as opposed to quadrilateral elements that are of the same size (Frei, 2021). However, it was decided that this reduced efficiency is outweighed by the increased geometrical accuracy.

3.2. Convergence study

To find the optimum element size to be used, a convergence study was conducted over a range of element sizes, using the Von-Mises stress at point C on Figure 2 as a reference point. Point C was chosen as it lies directly opposite to the applied force, and as such according to bending theory should experience a stress concentration (MechaniCalc., n.d). The stress at this node was recorded for a range of element sizes, of which the results can be seen in Figure 3.

From the study, the optimum element size was found using the largest size beyond which the scatter plot stayed within a 5 percent tolerance of the converged value. The converged value was found by averaging the stresses corresponding to the three smallest element sizes, and was found to be 12.01 MPa.

Using this method, the optimum mesh size was calculated to be 0.8mm, corresponding to a processing time of 60 seconds and a reference stress of 12.0248 MPa.

While a smaller mesh could have been selected, decreasing the mesh size further by 0.1mm would have led to a significant increase in computational time from 22.6 seconds to 29.6 seconds (31%) Corresponding to a relatively small change in Von-Mises stress, from 12.0248 MPa to 11.9963 MPa (0.003%). As such, it was decided that opting for a smaller mesh would not be justified.

Figure 3: A scatter plot of the FEA - computed reference stress against the number of elements in the model logged. Labelled in red is the point corresponding to optimum mesh size

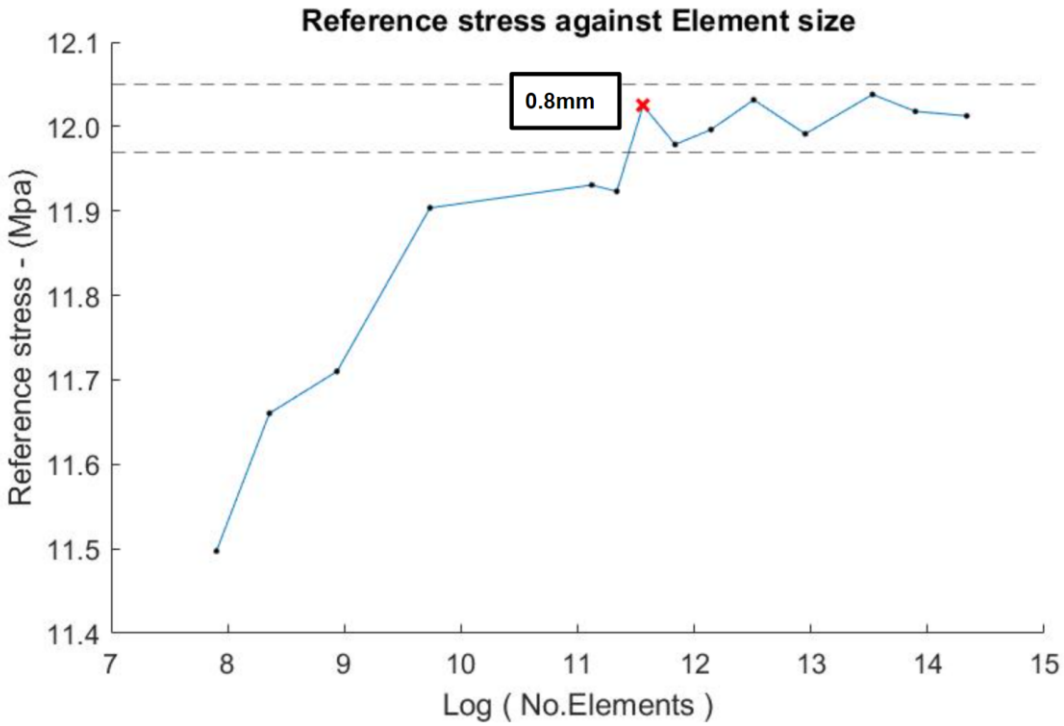

Part 4: Results

Using a parabolic triangular mesh with element size of 0.8mm, the FEA analysis was conducted, and a contour plot representing the Von-Mises stress distribution across the component was plotted.

This is shown overleaf in Figure 4, where it can be seen that there are three main areas of stress concentration; the left-most node that has been constrained, the location at which the point load has been applied, and the face directly opposing it. Stress was chosen as the parameter of interest as opposed to strain, as the latter is not crucial to measuring the component's performance.

While the maximum Von Mises stress was found to be 183 MPA, this was located at a constrained node. As such, it is unlikely to be accurate, and would need to be validated. Regardless, in comparing this to the yield strength of cast steel, 200MPa, it can be seen that the component should not fail by yielding. A similar observation can be made at the location of the point load, at which there is a reading of 126MPa.

Excluding these two stress concentrations, the largest stress experienced at the concentration directly opposite to the point load is 12MPa. Again, this lies comfortably within the yield strength of cast steel.

Figure 4: Contour plot of the Von Mises stress distribution of the final FEA model, representing half a squat-rack support bar under a 1500N point load

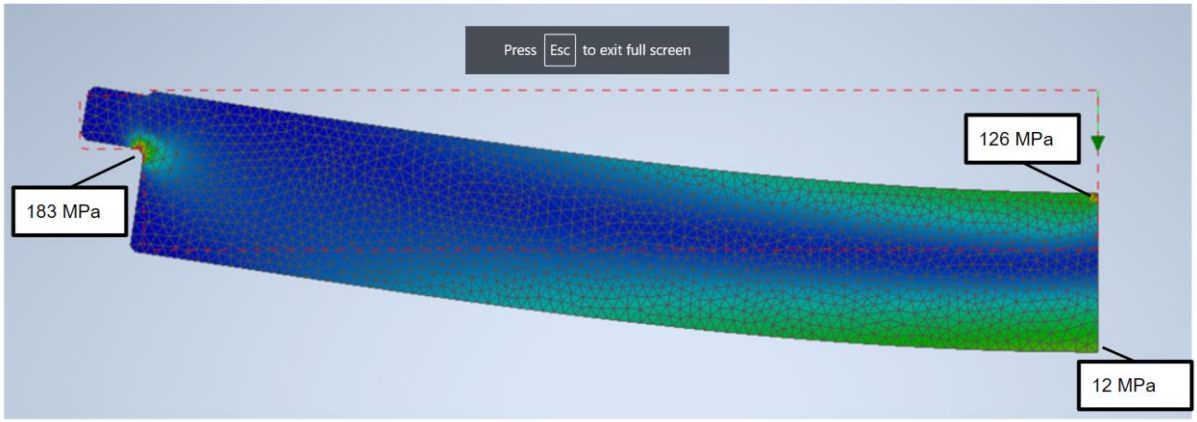

Part 5: Validation/Verification

In order to validate the FEA model, a possible approach would be to use an adapted version of a three point flexural test, as illustrated below in Figure 5.

With the bar supported at either end of the rig, a point load equivalent to 1500N would then be exerted at the centre of the bar. Placing strain gauges at the regions of interest identified in the FEA model, one could then use the strain measured to calculate the stress using the standard beam equations.

Figure 5: Schematic diagram describing a possible method of testing the safety bar under load

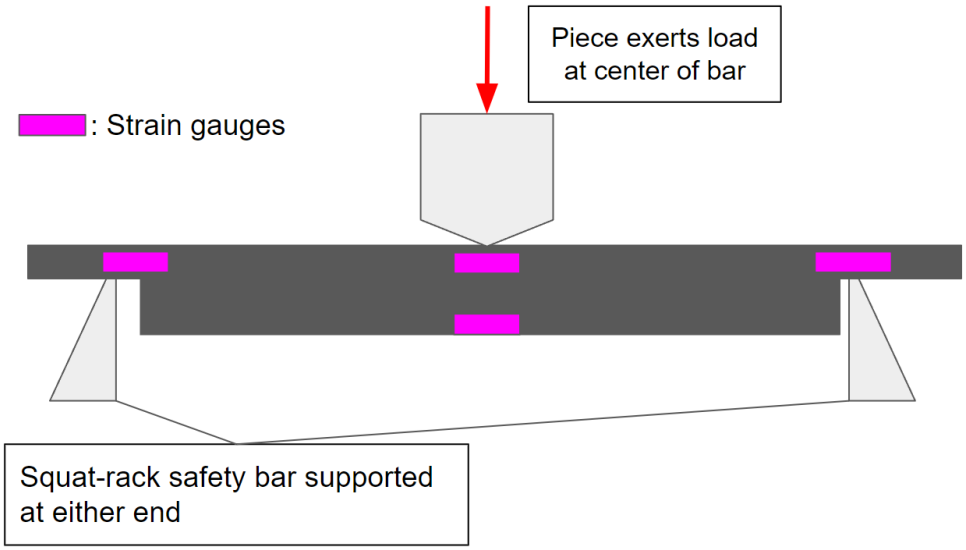

Part 6: Discussion

Generally, the solution produced by the FEA model can be considered accurate in the context of its boundary conditions. The use of a parabolic mesh ensures accuracy by increasing the number of nodes, while a triangular element shape ensures accuracy through better representing the geometry of the component's sharp corners.

Using a convergence study, an element size of 0.8mm was found to be appropriate, as it lies within the 5% tolerance threshold, without using an excessive amount of computational power and time. While the element size could be reduced to increase accuracy, it would result in an exponential increase in computational costs.

The model has several limitations due to its 2D plane stress idealisation. Firstly, the use of a point load and fixed point boundary condition limits the reliability of the results found at the points interest near them. Secondly, the bar has been assumed to be of constant thickness, while there is in fact a difference in thickness in its main section and its protrusions. Finally, the component's material properties were assumed to be that of cast steel, and isotropic. It is as such not a perfect representation of true material properties.

Regardless, the largest limitation of this model is that it is highly restricted in its application. The boundary conditions were assigned assuming a loading condition of a constant load acting at the centre of the bar. While this is a possible loading condition, it is unlikely to be relevant when evaluating the support bar's performance. In reality, the safety bar would be exposed regularly to unsymmetrical loading, high impact loads/ shocks from dropping weights, and fatigue. As such, this FEA model is both insufficient and inappropriate for determining if the support bar would fail in its working environment, and a more appropriate model would be needed.

In conclusion, while the FEA model can be said to be accurate within the context of its boundary conditions, it might still be improved, possibly using a smaller mesh size, or redefining the point load boundary constraint as a uniformly distributed load across a small section of the face. However, this would be unlikely to yield any data of useful application, as in reality, the component would be subject to a much wider range of loading conditions.

References

1. LIFEFITNESS., 2021. *Hammer Strength: HD Elite Power Rack* [Online]. Available from: <https://www.lifefitness.co.uk/en-gb/catalog/strength-training/racks-rigs/hammer-strength/hd-elite-power-rack> [Accessed 6 November 2022].

2. Pegg, E., 2022. *ME30030 Structural Mechanics*. University of Bath. Unpublished.

3. Poirier-Leroy, O., n.d. *The Ultimate Guide to Power Racks* [Online], Date posted. Available from: < https://www.yourworkoutbook.com/ultimate-guide-power-racks> [6 November 2022].

4. THOMASNET., n.d. *Material Properties of Iron and Steel Castings* [Online]. Thomas Publishing Company. Available from: <https://www.thomasnet.com/articles/custom-manufacturing-fabricating/material-properties-of-iron-and-steel-castings/> [Accessed 6 November 2022].

5. The Engineering Toolbox., n.d. *Poissons Ratio* [Online]. Available from: <https://www.engineeringtoolbox.com/poissons-ratio-d_1224.html> [10 November 2022].

6. Civil's Guide., 2021. *What is the Young's Modulus of Steel?* [Online]. Available from: URL [10 November].

7. Haimes, R., Docampo-Sánchez, J., 2019. *Toward Regular Quad-Mesh Generation*. Cambridge, MA: Massachusetts Institute of Technology. Available from: <https://acdl.mit.edu/ESP/Publications/AIAApaper2019-1988.pdf> [Accessed 8 November 2022].

8. Frei, W., 2021. *Meshing Your Geometry: When to Use the Various Element Types*. [Blog] COMSOL, Available at: <https://uk.comsol.com/blogs/meshing-your-geometry-various-element-types/> [Accessed 14 November 2022].

9. MechaniCalc., n.d. *Stresses and Deflections in Beams* [Online]. Available from: < https://mechanicalc.com/reference/beam-analysis > [Accessed 15 November 2022].